Multispectral optoacoustic tomography of benign and malignant thyroid disorders - a pilot study

Wolfgang Roll[1]*, Niklas A. Markwardt[2,3]*, Max Masthoff[4], Anne Helfen[4], Jing Claussen[5], Michel Eisenblätter[4,6], Alexa Hasenbach[7], Sven Hermann[7], Angelos Karlas[2,3], Moritz Wildgruber[4,8], Vasilis Ntziachristos[2,3]*, Michael Schäfers[1,7,8]*

[1] Department of Nuclear Medicine, University Hospital Münster, Germany

[2] Institute of Biological and Medical Imaging, Helmholtz Zentrum München, Germany

[3] Chair of Biological Imaging and TranslaTUM, Technische Universität München, Germany

[4] Institute of Clinical Radiology, University Hospital Münster, Germany

[5] iThera Medical, Munich, Germany

[6] Division of Imaging Sciences and Biomedical Engineering, King's College London, London, United Kingdom.

[7] European Institute for Molecular Imaging, University of Münster, Germany

[8] Cells in Motion (CiM) Cluster of Excellence, University of Münster, Germany

* These authors contributed equally to this work.

Corresponding author:

Wolfgang Roll, MD

Department of Nuclear Medicine, University Hospital Münster, Germany

Albert-Schweitzer-Campus 1, 48149 Münster, Germany

E-Mail: wolfgang.roll@ukmuenster.de

Telephone: +49 251 83 47362

Fax: +49 251 83 47360

Word Count: 2444

Funding: This study was supported in part by the IZKF Münster, project Z04 & Core Unit PIX. WR was funded by a rotational clinician scientist position of the Medical Faculty, University of Münster, Germany. NM has received funding from the European Union's Horizon 2020 research and innovation programme under grant agreement No 667933 (MIB) and AK by the Deutsche Forschungsgemeinschaft (DFG), Sonderforschungsbereich-824 (SFB-824), subproject A1. The research leading to these results has received additional funding from the Deutsche Forschungsgemeinschaft (DFG), Germany [Gottfried Wilhelm Leibniz Prize 2013; NT 3/10-1].

Conflict of interest: JC is an employee of iThera Medical, München. VN is a stakeholder of iThera Medical, München. No other potential conflicts of interest relevant to this article exist.

Short running title: optoacoustic imaging of the thyroid

ABSTRACT

This study aims at evaluating hybrid multispectral optoacoustic tomography (MSOT)/ultrasound for imaging of thyroid disorders, including Graves' disease and thyroid nodules. The functional biomarkers and tissue parameters deoxygenated (HbR), oxygenated (HbO2) and total hemoglobin (HbT), saturation of hemoglobin (sO2), fat and water content were analyzed in thyroid lobes affected by Graves' disease (n=6), thyroid lobes with healthy thyroid tissue (n=8), benign (n=13) and malignant (n=3) thyroid nodules. In Graves' disease, significantly higher values for HbR (3.18 ± 0.52 vs. 2.13 ± 0.62; p=0.0055) and HbT (8.34 ± 0.88 vs. 6.59 ± 1.16; p=0.0084) and significantly lower values for fat (0.64 ± 0.37 vs. 1.69 ± 1.25; p=0.0293) were found compared to healthy controls. Malignant thyroid nodules showed significantly lower sO2 (55.4% ± 2.6% vs. 60.8% ± 7.2%; p = 0.0393) and lower fat values (0.62 ± 0.19 vs. 1.46 ± 0.87; p=0.1295) than benign nodules. This pilot study shows the applicability and the potential of hybrid MSOT/ultrasound to semi-quantitatively provide tissue characterization and functional parameters in thyroid disorders for improved non-invasive diagnostics of thyroid diseases. [174 words]

Key Words

Multispectral optoacoustic tomography (MSOT), Graves' disease, thyroid nodule, hemoglobin

INTRODUCTION

Thyroid disorders including autoimmune diseases and thyroid nodules are common diseases worldwide. Graves' disease is one of the most frequent causes for hyperthyroidism, causing an antibody-mediated (autoimmune) inflammation of the thyroid gland (*1*,*2*). Clinical evaluation and risk stratification includes laboratory testing of thyroid hormones (TSH, fT3, fT4), autoantibodies (TRAK) and ultrasound/Doppler imaging (*2*). Tc-99m-scintigraphy is not recommended for routine monitoring of Graves' disease due to the related radiation exposure (*2*). Non-invasive and more specific functional monitoring of inflammatory activity as for example through multispectral optoacoustic tomography (MSOT) could establish an improved assessment of treatment response.

Thyroid nodules are detected in 19-68% of individuals by high-resolution ultrasound (*3*,*4*). Grading following American thyroid association guidelines (*5*), thyroid imaging reporting and documentation system (TIRADS) criteria (*6*) or modified TIRADS criteria (*7*) helps to estimate the risk of malignancy based on ultrasound patterns and nodule sizes guiding fine-needle aspiration (FNA). Providing a low number of false-negative results, FNA is a powerful diagnostic tool for non-surgical diagnosis (*2*). However, about 25% of thyroid nodules are classified as indeterminate and cannot be specified whether being benign, malignant, or suspicious for malignancy with a high risk of cancer (*8*). Definite conclusions can only be drawn from histopathology after (hemi-)thyroidectomy (*9*,*10*). Further evaluation and risk stratification imaging techniques such as the recently established elastography can be applied; however, these are operator-dependent and of highly variable performance (*5*). New non-invasive techniques like MSOT assessing functional tissue parameters might provide new biomarkers, which would be highly desirable to further assess risk patterns of individual thyroid nodules without the need for invasive procedures.

MSOT is based on the detection of ultrasonic waves generated by thermoelastic expansion of tissue illuminated with ultrashort laser pulses (Fig. 1) (*11*). Distributions of different tissue parameters, e.g. fat and water content or concentration of de- or oxygenated hemoglobin, can be calculated due to their specific intrinsic absorption properties. Recently, first potential clinical applications for optoacoustic imaging in the fields of vascular imaging (*12*,*13*), inflammatory bowel diseases (*14*) and oncology (*15*) have been reported. Regarding thyroid diseases, initial results of optoacoustic imaging *ex vivo* (*16*,*17*) recently triggered first proof of concept imaging studies of healthy subjects (*18*) and patients with thyroid nodules *in vivo* (*19*). However, both studies only applied one illumination wavelength implying that the spectral signatures of different tissue absorbers could not be used to quantify functional parameters in thyroid disorders. In addition, the integration of MSOT with ultrasound imaging being a current major imaging modality in clinical diagnostics of the thyroid – as implemented in the hybrid device used in this study – allows benefiting from both functional (through MSOT) and anatomical (through ultrasound) information co-registered in space and time.

The aim of this study is to evaluate the applicability and the potential of hybrid MSOT/ultrasound imaging in common disorders of the thyroid gland in patients compared to healthy controls. Functional tissue parameters provided by MSOT are used to assess inflammatory activity in Graves' disease and to further characterize thyroid nodules.

MATERIALS AND METHODS

Patients and Study Design

18 patients (median age 52, range 21-82 years) were included, consisting of Graves' disease patients (n=3) (Table 1), healthy volunteers (n=3), patients with only benign thyroid nodules (n=9) and patients with a malignant thyroid nodule (n=3).

For the comparison of Graves' disease with healthy thyroid tissue, fourteen thyroid lobes (Graves' disease: n=6; healthy tissue n=8) were included in this retrospective analysis. Lobes affected by Graves' disease (n=6) consisted of both lobes (left, right) of Graves' disease patients. Healthy tissue lobes (n=8) included one or two lobes per healthy volunteer (n=4) and contralateral, unaffected lobes of thyroid nodule patients (n=4). The two other lobes of healthy volunteers were excluded due to the presence of small cystic lesions. 16 thyroid nodules were analyzed, consisting of 13 benign (Supplemental Table 1) and three malignant nodules (Table 2). All patients underwent routine clinical thyroid evaluation in our nuclear medicine outpatients' clinic. Graves' disease evaluation included medical history, laboratory testing of thyroid hormones (TSH, fT3, fT4), autoantibodies (TRAK) and ultrasound with Doppler imaging following international guidelines (*2*). Risk stratification of thyroid nodules included ultrasound imaging, Tc-99m pertechnetate scintigraphy and, if recommended, FNA according to international guidelines was performed (*5*,*6*,*20*). Final diagnosis was based on histopathological results after thyroidectomy in four benign and three malignant nodules (Supplemental Table 1 and Table 2, respectively). FNA served as gold standard in four nodules. Hyperfunctional nodules with high uptake in Tc-99m pertechnetate scintigraphy were regarded as benign (n=5) and did not require FNA (*5*).

All patients and healthy subjects gave written and informed consent prior to enrolment. This retrospective analysis was approved by the institutional review board (2018-745-f-S).

Technical Aspects of MSOT Imaging Device

We used a hybrid clinical MSOT/ultrasound imaging system (MSOT Acuity Echo, iThera Medical, Munich, Germany) previously described in detail elsewhere (*15*,*21*). Laser excitation pulses had a duration of 9 ns with a repetition rate of 25 Hz. The pulse energy was attenuated to ensure adherence with American National Standards Institute limits of maximum permissible exposure (energy density below 20 mJ/cm^2). The detector (256 transducer elements with a center frequency of 3 MHz; send/receive bandwidth = 56%; optoacoustic resolution ~250 µm) had a 125° angular coverage providing 2D cross-sectional images with a field of view of 40 × 40 mm^2 and a reconstructed pixel size of 100 µm. Multispectral data were acquired using one pulse per wavelength. Reflection ultrasound computed tomography mode ultrasound images were generated as previously described (*15*).

MSOT Image Acquisition

MSOT imaging of the thyroid gland was conducted after routine clinical thyroid evaluation in our outpatients' clinic on the same day. Scans were performed at room temperature in stable conditions with the patient in identical supine position as in routine ultrasound imaging. Image acquisition took about 5 minutes with the handheld probe (see Fig. 1A) being in touch with the skin most of the time. While acquiring images of different wavelengths, the probe was placed transversally and longitudinally centered on the biggest extent of the thyroid lobe (Graves' disease, healthy lobe) or on the thyroid nodule. Breathholding was required. The eyes of examiners and patients were protected with laser safety goggles (protection level DIR LB3; wavelength range: 645-1400 nm; visible light transmission 40%). Examiners were experienced in head and neck/thyroid ultrasound as well as clinical optoacoustic imaging.

MSOT images were acquired at eight wavelengths ranging from 700 nm to 950 nm (700 nm, 730 nm, 760 nm, 800 nm, 850 nm, 900 nm, 920 nm, 950 nm).

Image Reconstruction and Data Analysis

MSOT images were reconstructed using a model-based algorithm with Tikhonov regularization and non-negativity constraint (*22*) after band-pass filtering (Chebyshev) between 90 kHz and 6 MHz and deconvolution with the electrical impulse response of the transducer. A single, effective speed of sound of 1510 m/s was assumed for tissue and coupling medium (heavy water). This reconstruction method was used to ensure optimal co-registration of MSOT and ultrasound images.

Individual contributions of the absorbers oxygenated (HbO2) and deoxygenated (HbR) hemoglobin, fat and water were recovered from the acquired data based on their spectral absorption characteristics by linear unmixing. For the unmixing of HbO2 and HbR, only the wavelengths 700 nm, 730 nm, 760 nm, 800 nm and 850 nm were used; for fat and water all abovementioned wavelengths (i.e. also 900 nm, 920 nm and 950 nm). Subsequently, total hemoglobin (HbT = HbO2 + HbR) and oxygen saturation (sO2 = HbO2/HbT) were calculated.

To increase the signal-to-noise ratio, 2-3 frame stacks representing different time intervals in the image sequence of a scan were evaluated and averaged. The time intervals were chosen to exhibit no significant detector or patient movement. Each frame stack was composed of five sequential multispectral frames, each consisting of eight single-wavelength slices (see Fig. 1B).

Regions of interest (ROI) were drawn in ultrasound images and transferred to the corresponding co-registered MSOT images. The pixelwise calculated unmixed absorber

concentrations were averaged in the regions of interest. In healthy tissue lobes and Graves' disease lobes, the ROIs were placed surrounding the whole lobe visible in the ultrasound image (see Fig. 1C as an example). In patients with thyroid nodules, the ROIs were placed surrounding the entire nodule (see Figs. 3A and 3B as an example) by a nuclear medicine specialist.

Statistical analysis was performed with MATLAB (Version R2017b, TheMathWorks, Inc., Natick, MA, USA). Grouped data were compared using the following scheme: In case both groups were normally distributed, a Student's t-test (for equal variances) or a Welch test (for different variances) was used. If at least one of the groups was not normally distributed, a Wilcoxon-Mann-Whitney test was applied. Results are indicated in the text as mean values ± one standard deviation and visualized in the figures as single points (Graves' disease/healthy tissue: single lobes; nodules: single nodules) with additional boxes indicating ± one standard deviation and additional lines representing the respective means. P values < 0.05 were considered significant.

RESULTS

Hybrid MSOT/ultrasound was as easily applicable to patients with thyroid diseases and controls as ultrasound alone, however requiring laser safety googles, allowing for non-invasive and semi-quantitative analysis of functional parameters integrated with anatomical information. These parameters were also sufficiently reproducible: The relative standard deviations referring to the 2-3 frame stacks used for the evaluation of each scan (see Methods, data analysis), averaged over all scans, remained below 10% (HbR: 4.9%, HbO2: 9.1%, HbT: 5.9%, sO2: 4.4%, water: 6.4%), or at least below 20% in the case of fat (16.1%). Similarly, contralateral lobes in healthy volunteers and Graves' disease patients showed similar results (as expected). Their deviations from the respective patient averages were reasonably small: 5.0%, 7.8%, 5.3%, 2.9%, 26.4% and 9.4% for HbR, HbO2, HbT, sO2, fat and water, respectively.

Graves' Disease

In Fig. 2A, HbR, HbT and fat images of healthy tissue and tissue affected by Graves' disease are exemplarily shown for one lobe of each group, highlighting the significant differences presented in Fig. 2B: In thyroid lobes affected by Graves' disease, HbR (3.18 ± 0.52; vs. 2.13 ± 0.62; p=0.0055)[1] and HbT (8.34 ± 0.88 vs. 6.59 ± 1.16; p=0.0084) values were significantly higher as compared to control tissue, whereas the fat content (0.64 ± 0.37 vs. 1.69 ± 1.25; p=0.0293) was significantly lower. HbO2, sO2 and water values did not differ significantly. Additionally, there were no significant differences in any of the six parameters between contralateral, unaffected lobes of thyroid nodule patients compared to lobes of healthy volunteers (both classified as healthy tissue).

Thyroid Nodules

The upper panel of Fig. 3 shows an exemplary capsulated benign nodule, which is well visible in MSOT. The dark (low-echo) rim in the raw ultrasound image (Fig. 3A) delineates the nodule. Drawing a ROI just along this rim (Fig. 3B) and transferring it to the MSOT image (sO2 image weighted with the total hemoglobin signal) helps identify the nodule as the region with comparably high sO2 (Fig. 3C).

Results of MSOT parameters in benign and malignant nodules are shown in Fig. 3D. A significant difference can be observed for sO2, which was lower in malignant (55.4% ± 2.6%) as compared to benign (60.8% ± 7.2%) nodules (p=0.0393). This difference would be

[1] Here and in the following, results are indicated as mean value ± one standard deviation.

even more striking without an outlier in the benign group with a remarkably low sO2 of about 40% (indicated by an arrow in Fig. 3D). This nodule was located just below a large blood vessel, which probably distorted the measured values. Furthermore, malignant nodules showed lower fat content (0.62 ± 0.19) than benign nodules (1.46 ±0.87), however not reaching statistical significance in the small patient sample of this pilot study (p=0.1295). HbO2, HbT and water values did not differ significantly.

DISCUSSION

Routine imaging of thyroid disorders includes ultrasound and if necessary further characterization with Tc-99m pertechnetate scintigraphy. Graves' disease can be diagnosed by clinical evaluation including laboratory testing and ultrasound imaging, especially Doppler perfusion imaging. The quantification of tissue parameters including HbR, HbO2, the related parameters HbT and sO2 as well as fat and water content using MSOT could provide additional important biomarkers for initial evaluation and differential diagnosis as well as therapy monitoring.

Higher values of HbR and HbT as well as lower fat content in Graves' disease tissue compared to healthy thyroid tissue as observed in our study are consistent with, however not specific for, the pathophysiology of an antibody-mediated inflammation of the thyroid with variable multifocal lymphocytic infiltrates (*23*). Graves' disease related hyperperfusion, a result of increased hormone production and stimulation of the thyroid and proven by Doppler imaging (*24*), is reflected in significantly higher HbT values in our study. In contrast to Doppler imaging, MSOT additionally allows the semi-quantitative analysis of different tissue parameters that are only partly related to blood flow, as for example sO2 and HbT. Significantly higher HbR values for Graves' disease tissue compared to healthy tissue, as seen in our results, consecutively underline the need for oxygen of the antibody-activated (TRAK) thyroid gland. The highly variable tissue remodeling process obviously depends on the current status of ongoing inflammation (TRAK, ultrasound/Doppler) and administration of anti-thyroidal drugs (*2*,*23*). In Graves' disease, the thyroid is characterized by follicular hyperplasia and reduction in follicular colloid, which can potentially explain the significantly lower fat content compared to healthy tissue in our study. By assessing such functional tissue markers, MSOT could establish a non-invasive insight into ongoing inflammation and tissue remodeling of the thyroid gland in Graves' disease not possible with ultrasound/Doppler imaging. Together with state-of-the-art imaging (ultrasound/Doppler; scintigraphy), laboratory testing and clinical evaluation, additional assessment of functional tissue markers by MSOT could support initial evaluation and therapy monitoring in Graves' disease patients.

Thyroid nodules are common and their pathophysiological differentiation (benign/malignant) remains challenging while differentiated thyroid cancer becomes increasingly prevalent (*5*). Following international guidelines, thyroid nodules can be non-invasively graded based on ultrasound patterns (*5*,*9*,*10*). The use of Doppler imaging is not routinely recommended for risk stratification of thyroid nodules (*6*,*7*), however, it can help to distinguish between different tissues and to detect the limits of a nodule. New functional parameters assessed by MSOT, going beyond perfusion imaging with Doppler, might help to introduce new biomarkers/risk factors for risk stratification. In line with preliminary results

ex vivo (*16*), malignant nodules, although only constituting a quite small group (n=3) in our pilot study, exhibited significantly lower sO2 values than benign nodules. These lower sO2 values could reflect increased oxygen consumption by malignant nodules resulting in neovascularization. The resulting small vessels were reported to be detected with higher sensitivity in optoacoustic imaging than in Doppler ultrasound (*18*,*19*). Lower fat content of malignant nodules in the previous study *ex vivo* (*16*) could also be reproduced in our study *in vivo*, possibly reflecting high cellularity of tumor tissue compared to benign nodules. The easily feasible, additional assessment of these functional biomarkers and tissue parameters by MSOT, combined with standard of care including risk stratification of thyroid nodules by ultrasound and FNA, could support clinical grading and follow-up of thyroid nodules. Its value for and position in the multimodal algorithm of risk assessment of thyroid nodules (*5*–*7*) needs to be defined in larger prospective studies.

The large standard deviations of the MSOT parameters of malignant nodules for HbR, HbO2 and HbT may be due to the low number of malignant nodules included in this pilot study, their different tumor stages, levels of aggressiveness and tumor sizes (Table 2), as well as technical limitations. Benign nodules are a very heterogeneous group as well, ranging from restrictive adenoma with high cellularity to hyperfunctional, fast-growing nodules with cystic components.

A further limitation of this pilot study is the comparably limited number (eight) of wavelengths used for data acquisition. Newest developments allow the application of significantly more (e.g. 28) wavelengths within an acceptable time window, resulting in more reliable spectral unmixing. Currently, MSOT is still prone to several artefacts originating e.g. from the limited view of the probes and from perturbations from overlaying tissue as for instance large blood vessels producing high MSOT signal. Advances in the technology of handheld optoacoustic devices, image reconstruction and unmixing algorithms are needed to overcome current limitations.

In conclusion, we present first evidence for the applicability and the diagnostic potential of hybrid MSOT/ultrasound imaging in thyroid disorders. Larger prospective studies are needed to corroborate our observations.

REFERENCES

1. Léger J, Carel JC. Diagnosis and management of hyperthyroidism from prenatal life to adolescence. *Best Pract Res Clin Endocrinol Metab*. 2018;32:373-386.
2. Ross DS, Burch HB, Cooper DS, et al. 2016 American Thyroid Association Guidelines for Diagnosis and Management of Hyperthyroidism and Other Causes of Thyrotoxicosis. *Thyroid*. 2016;26:1343-1421.
3. Tan GH, Gharib H. Thyroid incidentalomas: Management approaches to nonpalpable nodules discovered incidentally on thyroid imaging. *Ann Intern Med*. 1997;126:226-231.
4. Guth S, Theune U, Aberle J, Galach A, Bamberger CM. Very high prevalence of thyroid nodules detected by high frequency (13 MHz) ultrasound examination. *Eur J Clin Invest*. 2009;39:699-706.
5. Haugen BR, Alexander EK, Bible KC, et al. 2015 American Thyroid Association Management Guidelines for Adult Patients with Thyroid Nodules and Differentiated Thyroid Cancer: The American Thyroid Association Guidelines Task Force on Thyroid Nodules and Differentiated Thyroid Cancer. *Thyroid*. 2016;26:1-133.
6. Tessler FN, Middleton WD, Grant EG, et al. ACR Thyroid Imaging, Reporting and Data System (TI-RADS): White Paper of the ACR TI-RADS Committee. *J Am Coll Radiol*. 2017;14:587-595.
7. Russ G, Bonnema SJ, Erdogan MF, Durante C, Ngu R, Leenhardt L. European Thyroid Association Guidelines for Ultrasound Malignancy Risk Stratification of Thyroid Nodules in Adults: The EU-TIRADS. *Eur Thyroid J*. 2017;6:225-237.
8. Poller DN, Baloch ZW, Fadda G, et al. Thyroid FNA: New classifications and new interpretations. *Cancer Cytopathol*. 2016;124:457-466.
9. Chaigneau E, Russ G, Royer B, et al. TIRADS score is of limited clinical value for risk stratification of indeterminate cytological results. *Eur J Endocrinol*. 2018;179:13-20.
10. Schenke S, Zimny M. Combination of Sonoelastography and TIRADS for the Diagnostic Assessment of Thyroid Nodules. *Ultrasound Med Biol*. 2018;44:575-583.
11. Ntziachristos V, Ripoll J, Wang L V., Weissleder R. Looking and listening to light: The evolution of whole-body photonic imaging. *Nat Biotechnol*. 2005;23:313-320.
12. Taruttis A, Timmermans AC, Wouters PC, Kacprowicz M, van Dam GM, Ntziachristos V. Optoacoustic Imaging of Human Vasculature: Feasibility by Using a Handheld Probe. *Radiology*. 2016;281:256-263.
13. Masthoff M, Helfen A, Claussen J, et al. Use of Multispectral Optoacoustic Tomography to Diagnose Vascular Malformations. *JAMA Dermatology*. 2018;154: 1457–1462.
14. Knieling F, Neufert C, Hartmann A, et al. Multispectral Optoacoustic Tomography for Assessment of Crohn's Disease Activity. *N Engl J Med*. 2017;376:1292-1294.
15. Becker A, Masthoff M, Claussen J, et al. Multispectral optoacoustic tomography of the human breast: characterisation of healthy tissue and malignant lesions using a hybrid ultrasound-optoacoustic approach. *European radiology*. 2018:602-609.
16. Dogra VS, Chinni BK, Valluru KS, et al. Preliminary results of ex vivo multispectral photoacoustic imaging in the management of thyroid cancer. *Am J Roentgenol*. 2014;202:552-558.
17. Kang J, Chung WY, Kang SW, et al. Ex Vivo estimation of photoacoustic imaging for detecting thyroid microcalcifications. *PLoS One*. 2014;9:e113358.
18. Dima A, Ntziachristos V. In-vivo handheld optoacoustic tomography of the human thyroid. *Photoacoustics*. 2016;4:65-69.

19. Yang M, Zhao L, He X, et al. Photoacoustic/ultrasound dual imaging of human thyroid cancers: an initial clinical study. *Biomed Opt Express*. 2017;8:3449.
20. Cross P, Chandra A, Giles T, et al. Guidance on the reporting of thyroid cytology specimens January 2016. Royal College of Pathologists. https://www.rcpath.org/uploads/assets/uploaded/9ddf3c1d-c58f-4b8c-b89b63e0704f5a50.pdf.
21. Masthoff M, Helfen A, Claussen J, et al. Multispectral optoacoustic tomography of systemic sclerosis. *J Biophotonics*. 2018;11:e201800155.
22. Ding L, Luís Deán-Ben X, Lutzweiler C, Razansky D, Ntziachristos V. Efficient non-negative constrained model-based inversion in optoacoustic tomography. *Phys Med Biol*. 2015;60:6733-6750.
23. McIver B, Morris JC. The pathogenesis of graves' disease. *Endocrinol Metab Clin North Am*. 1998;27:73-89.
24. Ralls PW, Mayekawa DS, Lee KP, et al. Color-flow Doppler sonography in Graves disease: "Thyroid inferno." *Am J Roentgenol*. 1988;150:781-784.

FIGURES

FIGURE 1

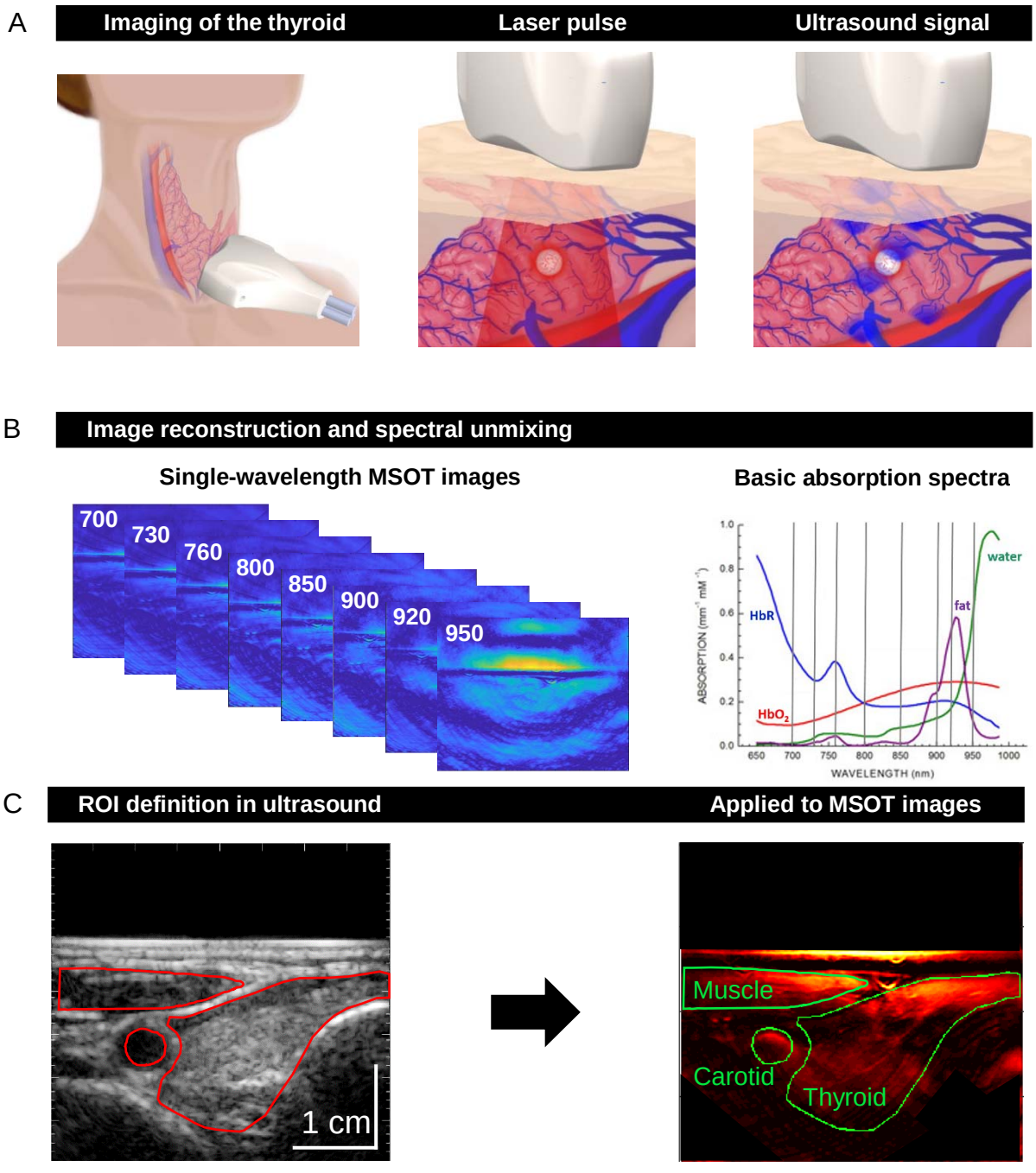

Principles of clinical MSOT of the thyroid

A: Scheme of an examination of the thyroid gland with a handheld hybrid multispectral optoacoustic tomography (MSOT) / ultrasound system (left). Patients with thyroid nodules, healthy individuals and Graves' disease patients were scanned in a reproducible setup. Optoacoustic imaging is based on the absorption of irradiated laser pulses within the tissue

(middle), followed by thermoelastic expansion and the induction of ultrasound waves that can be detected with a handheld detector (right).

B: In a first step, MSOT images are acquired for single wavelengths (left). Spectral unmixing, based on specific absorption spectra of different tissue constituents (right), allows the assessment of functional parameters like deoxygenated (HbR) and oxygenated (HbO2) hemoglobin, fat and water.

C: Transversal ultrasound image of the thyroid gland and surrounding tissue allows the exact localization of anatomic structures (left). The regions of interest drawn in ultrasound images were transferred to the coregistered pseudocolor-coded averaged MSOT images (here: HbT) for visual and quantitative analysis (right).

FIGURE 2

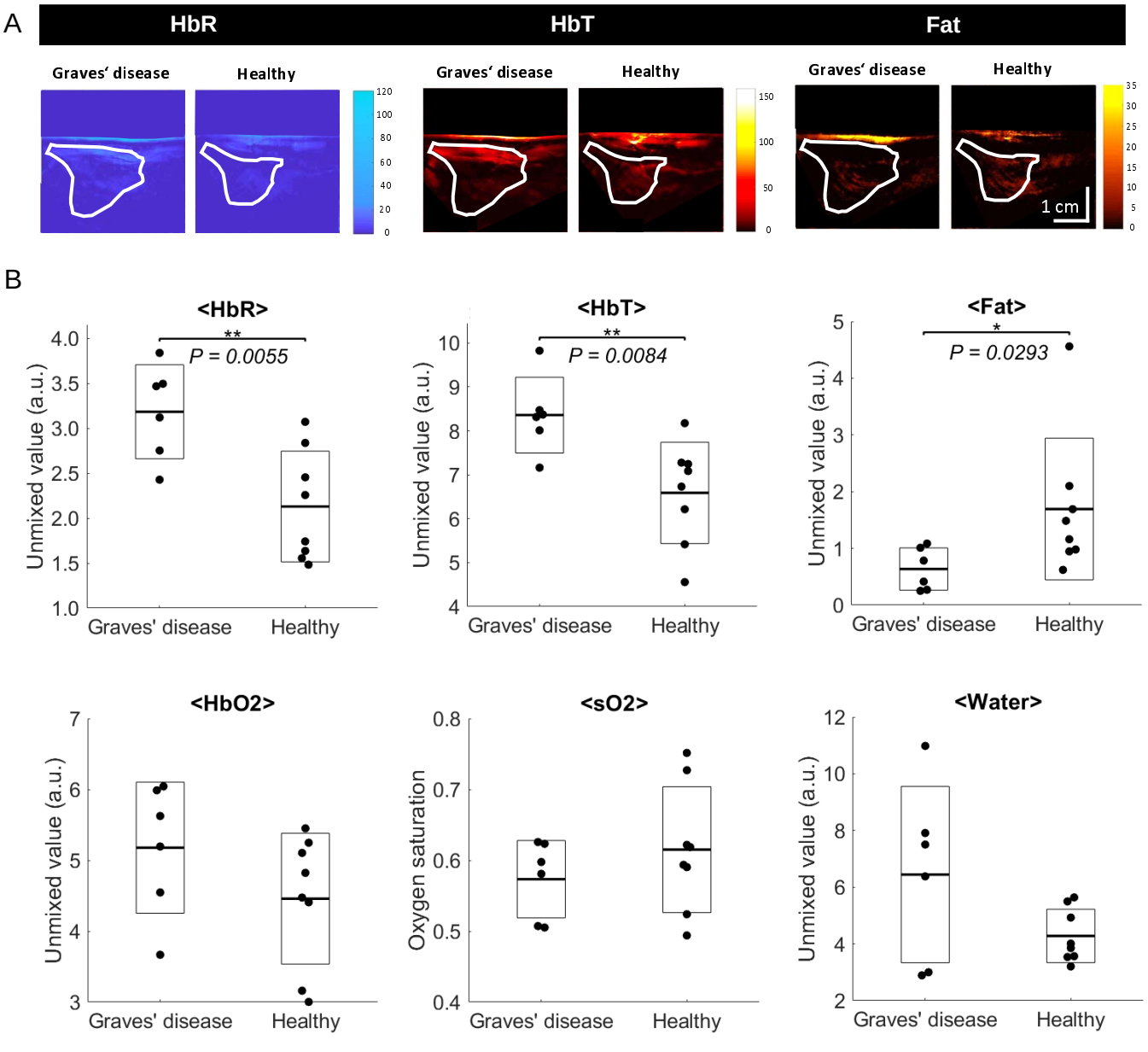

MSOT-derived functional markers of inflammatory activity in Graves' disease

A: Exemplary pseudocolor-coded MSOT images of HbR, HbT and fat of Graves' disease and healthy thyroid tissue. Images show higher HbR and HbT and lower fat contents in Graves' disease compared to healthy tissue. ROIs transferred from corresponding ultrasound images are shown to identify the localization of the investigated thyroid lobe.

B: Quantification of MSOT values for deoxygenated (HbR), oxygenated (HbO2) and total hemoglobin (HbT=HbR+HbO2), sO2 (HbO2/HbT), fat and water for thyroid lobes affected by Graves' disease and healthy thyroid tissue. Single thyroid lobes are represented by

single points with additional boxes indicating ± one standard deviation and additional lines representing the respective means. Graves' disease shows significantly elevated HbR and HbT values and significantly reduced fat values compared to healthy thyroid tissue (*$p<0.05$, **$p<0.01$).

FIGURE 3:

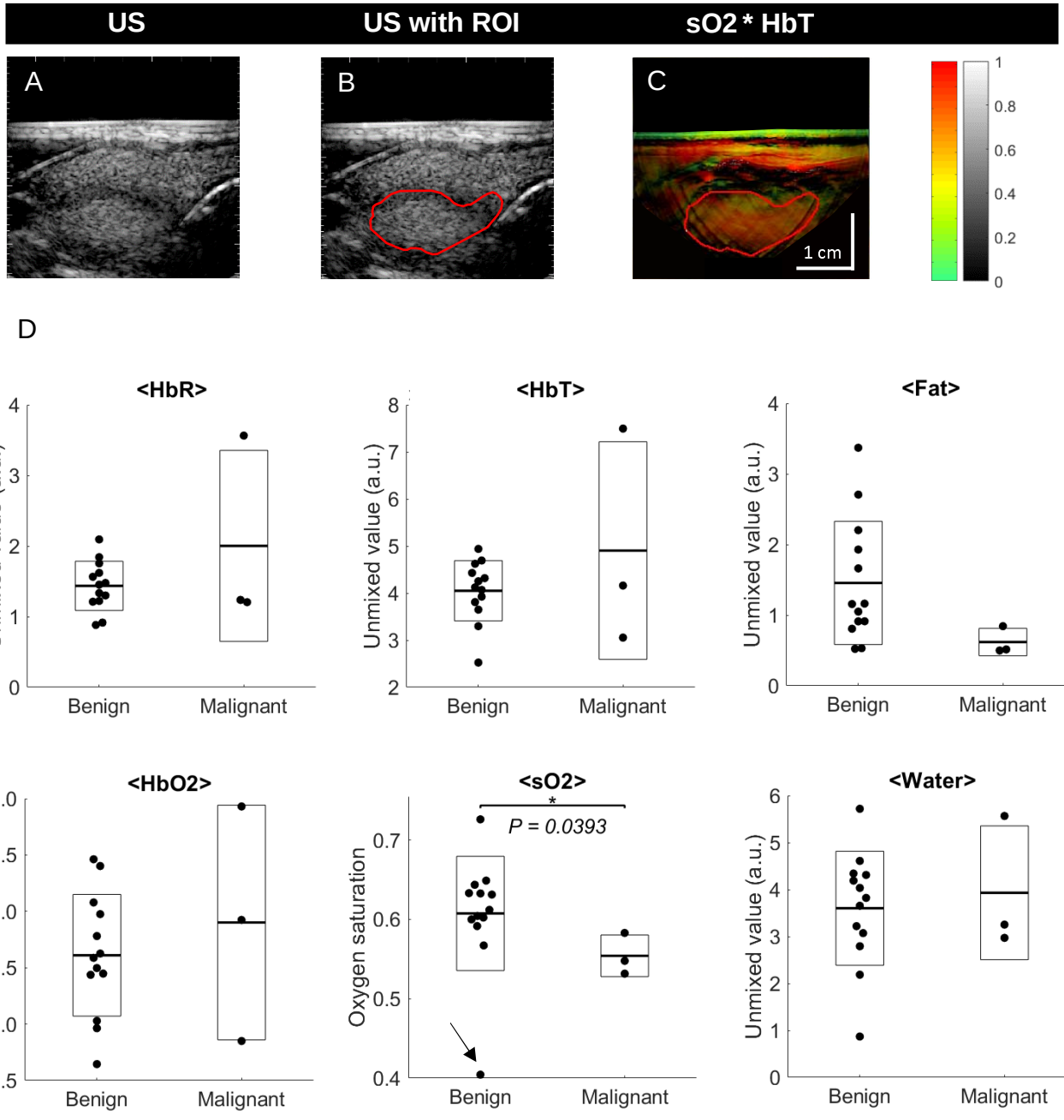

MSOT-derived functional markers in benign and malignant thyroid nodules

Exemplary images of a well-visible benign thyroid nodule in ultrasound (**A**) delineated by a ROI (**B**). Transfer to co-registered pseudocolored MSOT image of sO2 weighted with the signal of total hemoglobin (**C**) shows co-localization of the region with elevated sO2 values with the anatomical localization of the nodule.

D: Quantification of MSOT values for deoxygenated (HbR), oxygenated (HbO2) and total hemoglobin (HbT=HbR+HbO2), sO2 (HbO2/HbT), fat and water for benign and malignant

nodules. Single nodules are represented by single points with additional boxes indicating ± one standard deviation and additional lines representing the respective means. Malignant nodules show significantly reduced sO2 values compared to benign nodules (*$p<0.05$, **$p<0.01$). The arrow in the sO2 plot indicates an outlier discussed in the main text.

TABLES

TABLE 1.: Graves' Disease Patients Characteristics

Study ID	Age at diagnosis	Diagnosis	Thyroid volume [ml]	Doppler	fT3 [pg/ml] (2.3-4.2)	TRAK [U/l]	Thyreostatics/d
#1	45	Graves' disease	21	hyperperfused	4.9	12.3	10 mg Carbimazol
#2	21	Graves' disease	47	hyperperfused	11.2	8331.7	60 mg Carbimazol
#3	53	Graves' disease	17	hyperperfused	5.9	6.05	20 mg Thiamazol

Information on Graves' disease patients including patient age at diagnosis, imaging parameters (thyroid volume, Doppler), laboratory results (fT3, TRAK) and ongoing thyreostatic therapy.

TABLE 2.: Thyroid Carcinoma Patients Characteristics

Nodule	Age at diagnosis	Localization	Diagnosis	TNM (UICC 2010)	Size [cm]
#1	24	Right lobe	PTC	pT2	3.5
#2	21	Left lobe	PTC	pT1b	1.5
#3	66	Left lobe	PTC	pT1a	0.3

Information on malignant nodules including patient age at diagnosis, localization of the nodule, diagnosis with TNM classification and size of the tumor. PTC=papillary thyroid carcinoma

1

A

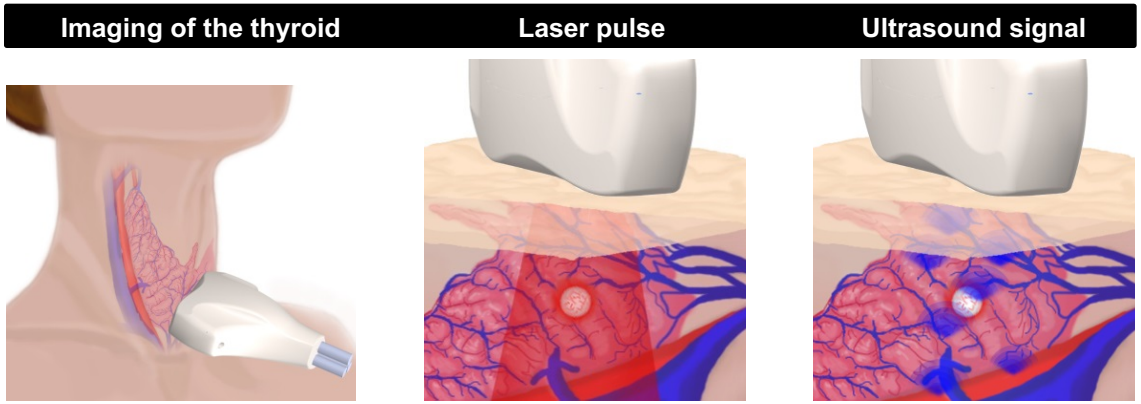
Imaging of the thyroid
Laser pulse
Ultrasound signal

B

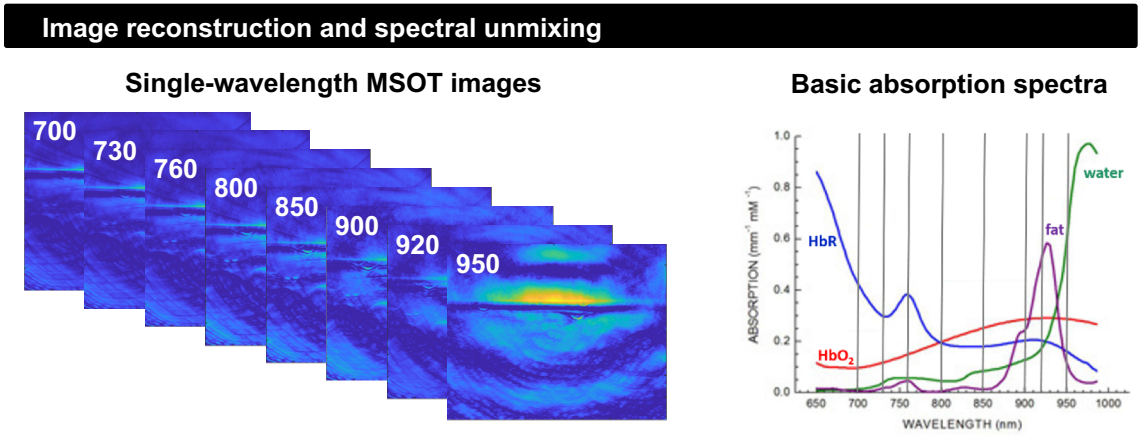
Image reconstruction and spectral unmixing
Single-wavelength MSOT images
700
730
760
800
850
900
920
950
Basic absorption spectra
ABSORPTION (mm⁻¹ mM⁻¹)
WAVELENGTH (nm)
HbR
HbO2
fat
water

C

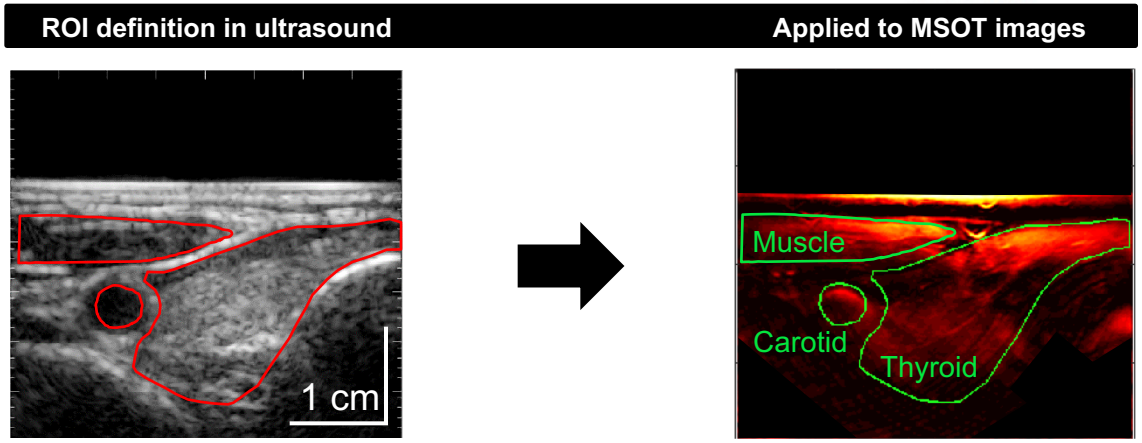
ROI definition in ultrasound
Applied to MSOT images
1 cm
Muscle
Carotid
Thyroid

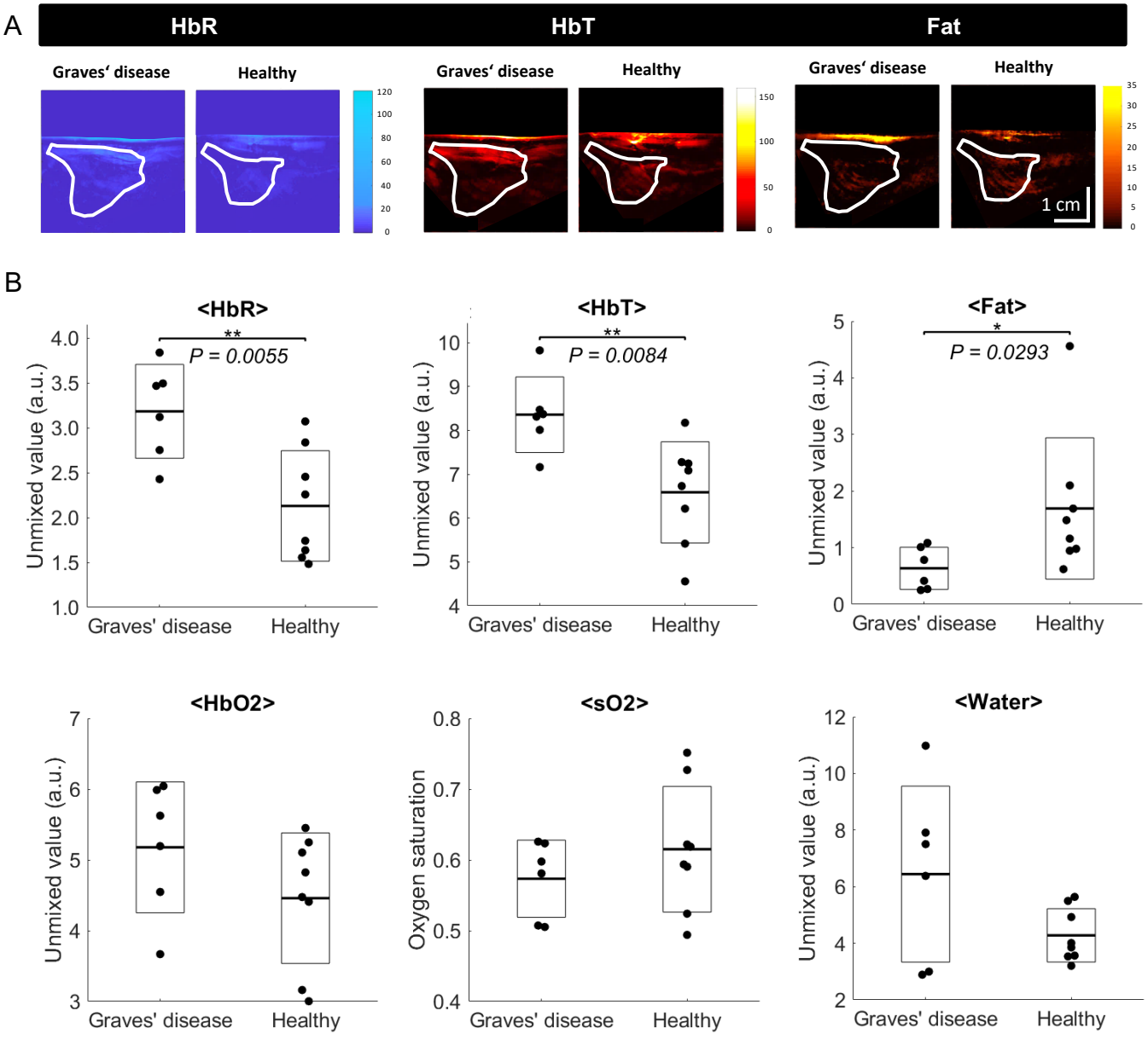
A
HbR
HbT
Fat
Graves' disease
Healthy
Graves' disease
Healthy
Graves' disease
Healthy
1 cm
B
<HbR>
**
P = 0.0055
Unmixed value (a.u.)
Graves' disease
Healthy
<HbT>
**
P = 0.0084
Unmixed value (a.u.)
Graves' disease
Healthy
<Fat>
*
P = 0.0293
Unmixed value (a.u.)
Graves' disease
Healthy
<HbO2>
Unmixed value (a.u.)
Graves' disease
Healthy
<sO2>
Oxygen saturation
Graves' disease
Healthy
<Water>
Unmixed value (a.u.)
Graves' disease
Healthy

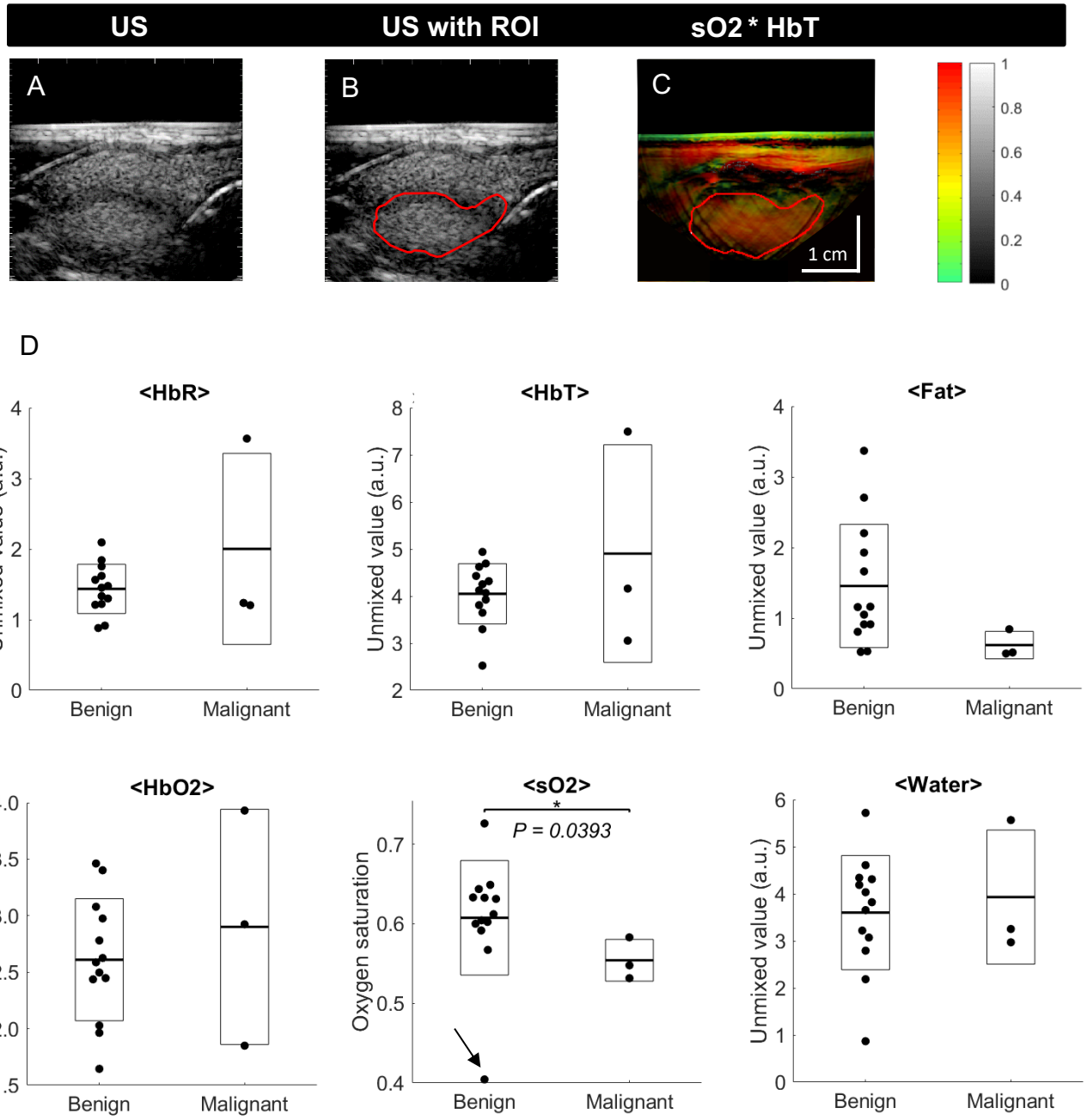
US
US with ROI
sO2 * HbT
A
B
C
1 cm
1
0.8
0.6
0.4
0.2
0
D
<HbR>
<HbT>
<Fat>
<HbO2>
<sO2>
<Water>
Unmixed value (a.u.)
Oxygen saturation
Benign
Malignant
*
P = 0.0393